Representing BRDF by Wavelet Transformation of Pair-Copula Constructions

Ahmet Bilgili*
International Computer Institute
Ege University

Aydın Öztürk†
Department of Computer Engineering
Yaşar University

Murat Kurt‡
International Computer Institute
Ege University

Abstract

Bidirectional Reflectance Distribution Functions (BRDFs) are well-known functions in computer graphics, and these special functions represent the surface reflectance of materials. BRDFs can be viewed as multivariate probability density function (pdf) of incoming photons leaving in a particular outgoing direction. However, constructing a multivariate probability distribution for modeling a given BRDF is difficult. A family of distributions, namely Copula distributions have been used to approximate BRDF. In this work, we employ the Pair-Copula constructions to represent the measured BRDF densities. As the measured BRDF densities have large storage needs, we use Wavelet transforms for a compact BRDF representation. We also compare the proposed BRDF representation with a number of well-known BRDF models, and show that our compact BRDF representation provides good approximation to measured BRDF data.

CR Categories: Computer Graphics [I.3.7]: Three-Dimensional Graphics and Realism—Color, shading, shadowing, and texture

Keywords: Copula distributions, BRDF representation, reflection models, rendering, global illumination, wavelet, pair-copula constructions

1 Introduction

Modeling the surface reflectance of light is an important issue in computer graphics. Expressing the surface reflectance by a mathematical model has been studied extensively. BRDFs are commonly used as mathematical models to describe the surface reflectance. BRDF was first formulated by Nicodemus et al. [1977] as

$$\rho(\vec{\omega}_i, \vec{\omega}_o) = \frac{dL_o(\vec{\omega}_o)}{L_i(\vec{\omega}_i)\cos\theta_i d\vec{\omega}_i}, \tag{1}$$

where $\rho(\vec{\omega}_i, \vec{\omega}_o)$ is the BRDF, L_i and L_o are the incident and reflected radiance, respectively, $(\vec{\omega}_i, \vec{\omega}_o) = \{(\theta_i, \phi_i), (\theta_o, \phi_o)\}$ are the corresponding incoming and outgoing vectors expressed in spherical coordinates using the elevation (θ) and azimuth (ϕ) angles, $d\vec{\omega}_i$ is the differential solid angle in the ω_i direction. Here radiance can be thought of as the pixel intensity at a given position of an image.

*e-mail: ahmetbilgili@gmail.com
†e-mail: aydin.ozturk@yasar.edu.tr
‡e-mail: murat.kurt@ege.edu.tr

It is noted that BRDF is the ratio of outgoing radiance $dL_o(\vec{\omega}_o)$ to incoming irradiance.

BRDF is defined only above the surface that is on the upper hemisphere. The support for the elevation angle is $[0, \pi/2]$ and for the azimuth angle is $[0, 2\pi]$ since the light transportation or the scattering below the surface is not considered.

The BRDF defined in Equation 1 is a four-dimensional (4D) function. The number of dimensions of the BRDF can be reduced if certain physical properties of the material surface can be assumed. If the reflection surface is assumed to be isotropic such as plastic, nickel, etc. then the corresponding BRDF can be expressed by a three-dimensional (3D) function. On the other hand, anisotropic surfaces such as velvet, brushed metal, etc. are represented by a 4D BRDF.

A physically correct BRDF representation must satisfy reciprocity, energy conservation, and non-negativity properties of BRDF [Edwards et al. 2006]. Reciprocity property is expressed as

$$\rho(\vec{\omega}_i, \vec{\omega}_o) = \rho(\vec{\omega}_o, \vec{\omega}_i), \tag{2}$$

where $\rho(\vec{\omega}_i, \vec{\omega}_o)$, $\vec{\omega}_i$, and $\vec{\omega}_o$ are described in Equation 1. Since our proposed model is based on the parameterization by Rusinkiewicz [1998], we enforce our system with the following translation to ensure reciprocity property

$$\phi_d = \phi_d + \pi, \tag{3}$$

where ϕ_d is azimuth angle of the difference vector described in Rusinkiewicz [1998] system. Therefore the proposed model is a visually plausible representation, since it only satisfies the reciprocity and non-negativity properties, but it does not guarantee energy conservation property.

Certain probabilistic properties of reflection have been used in various BRDF models including [Phong 1975; Blinn 1977; Cook and Torrance 1981; He et al. 1991; Ward 1992; Oren and Nayar 1994; Lafortune et al. 1997; Ashikhmin and Shirley 2000; Dür 2006]. Considering the energy conservation property of BRDF, Edwards et al. [2006] have proposed a bivariate probability BRDF, and Geisler-Moroder and Dür [2010] have made some modifications to Ward-Dür BRDF model [Dür 2006].

Aas et al. [2009] proposed a technique to model multivariate data using a cascade of pair-copulae, employing two variables at a time. In this paper, we adopted this technique to represent the BRDF. Furthermore, we used wavelet transforms proposed by Genest et al. [2009] to compress the pair-copula distributions. Our empirical results showed that the pair-copula constructions and wavelet transforms provided satisfactory approximations for the measured BRDF data.

2 Modeling BRDF by Probability Distributions

When a photon hits the surface of a material, it scatters from surface to a direction with a random distribution [Akenine-Möller et al.

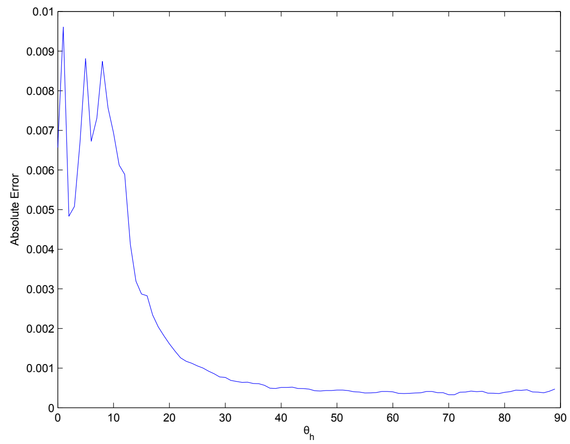

Figure 1: Absolute fitting errors on every θ_h of measured dark-red-paint material (red channel).

2008]. Considering certain probabilistic features of the underlying process, various models have been proposed to represent this random reflection. For example, Ward [1992] employed the Gaussian distribution to model bidirectional scattering of a given surface. Assuming that a material surface consists of microfacets, Cook and Torrance [1981] modeled the orientation of these microfacets using Beckmann distribution. Among the other factors, they included this univariate distribution in their BRDF model.

A different approach based on treating BRDF data in the context of probability theory was used by Edwards et al. [2006]. They modeled the BRDF in terms of a bivariate probability distribution. The underlying bivariate probability distribution was expressed as a function of the halfway vector which is defined as:

$$\vec{\omega}_h = \frac{\vec{\omega}_i + \vec{\omega}_o}{\|\vec{\omega}_i + \vec{\omega}_o\|}, \tag{4}$$

where $\vec{\omega}_i$ and $\vec{\omega}_o$ are the corresponding incoming and outgoing vectors.

Öztürk et al. [2010] have modeled BRDF data using Archimedean copula distributions. In their work, Archimedean copula distributions are represented by the corresponding empirical marginal distributions of BRDF data and some non-linear parameters. Their BRDF model is based on using a special parameterization of Rusinkiewicz [1998]. This parameterization is based on the halfway vector $\vec{\omega}_h = (\theta_h, \phi_h)$ and the difference vector $\vec{\omega}_d = (\theta_d, \phi_d)$. This BRDF parameterization aligns certain BRDF features with directions of certain BRDF phenomena [Lawrence et al. 2004; Ngan et al. 2005]. In this work, we adopted Aas et al. [2009]'s technique which is based on factorizing multivariate data using a cascade of pair-copulae, and does not require non-linear parameters. This makes our data fitting procedure more stable when compared to BRDF models proposed by [Blinn 1977; Cook and Torrance 1981; Lafortune et al. 1997; Öztürk et al. 2010]. All of these BRDF models require non-linear parameter estimation techniques in their data fitting process. We also applied wavelet transforms [Genest et al. 2009] to the pair-copula distributions for obtaining a compact BRDF representation.

A well-known measured data set [Matusik et al. 2003] was used for testing and comparison purposes. This data set includes 100 materials each of which requires 33 MB storage space. Rusinkiewicz [1998] parameterization was used to store the underlying measured BRDF data. Clearly, the size of the data is prohibitively large for rendering in a practical application. This problem can be overcome by employing a compact BRDF representation.

Measured BRDF data can be modeled by a multivariate probability distribution provided that an appropriate scaling transformation is performed on it. In the normalized BRDF, each scaled BRDF value is considered as an observed density of the scattered photon in a particular direction. In this work, we employed pair-copulae constructions to model the normalized BRDF data.

3 Pair-Copula Constructions

A copula distribution is a multivariate distribution with uniformly distributed $U(0,1)$ marginals. Copula distributions can isolate the description of the dependency structure of the joint distribution from its marginal distributions. Based on Sklar's theorem every multivariate distribution can be written as

$$\begin{aligned} F(x_1, x_2, ..., x_n) &= C\{F_1(x_1), F_2(x_2), ..., F_n(x_n)\} \\ &= C(u_1, u_2, ..., u_n), \end{aligned} \tag{5}$$

where C is the cumulative copula distribution function, $u_i = F_i(x_i), i = 1, 2, ..., n$ are the marginal distributions of joint distribution F [Nelsen 2006].

Joint density function f is given as:

$$f(x_1, x_2, ..., x_n) = c_{1\cdots n}\{F_1(x_1), F_2(x_2), ..., F_n(x_n)\} \prod_{i=1}^{n} f_i(x_i), \tag{6}$$

where $c_{1\cdots n}$ is the copula pdf and $f_i(x_i), i = 1, 2, ..., n$ are the marginal densities of joint pdf [Genest et al. 2009].

In this work, BRDF is considered as a joint density function of four variables. These variables are explained in Section 4. It is shown that BRDF can be factorized using a cascade of simple building blocks called pair-copulae [Aas et al. 2009]. In this section, we summarized their work for the sake of completeness.

The building blocks are based on the conditional independence. This independence of a multivariate pdf f can be shown with the following relationship:

$$f(x_1, x_2, ..., x_n) = f(x_n) f(x_{n-1}|x_n) \cdots f(x_1|x_2, ..., x_n). \tag{7}$$

For example if a two-dimensional (2D) case is considered, the pdf $f(x_1, x_2)$ can be written as:

$$f(x_1, x_2) = f_2(x_2) f(x_1|x_2). \tag{8}$$

If 2D pdf can be written in terms of copula density as,

$$f(x_1, x_2) = c_{12}\{F_1(x_1), F_2(x_2)\} f_1(x_1) f_2(x_2), \tag{9}$$

then the conditional pdf $f(x_1|x_2)$ can be written as:

$$f(x_1|x_2) = c_{12}\{F_1(x_1), F_2(x_2)\} f_1(x_1). \tag{10}$$

The factorization of a 3D pdf is not trivial. More than one alternative decompositions of the 3D density function can be obtained. The 3D pdf $f(x_1, x_2, x_3)$ can be expressed as

$$f(x_1, x_2, x_3) = f_3(x_3) f(x_2|x_3) f(x_1|x_2, x_3). \tag{11}$$

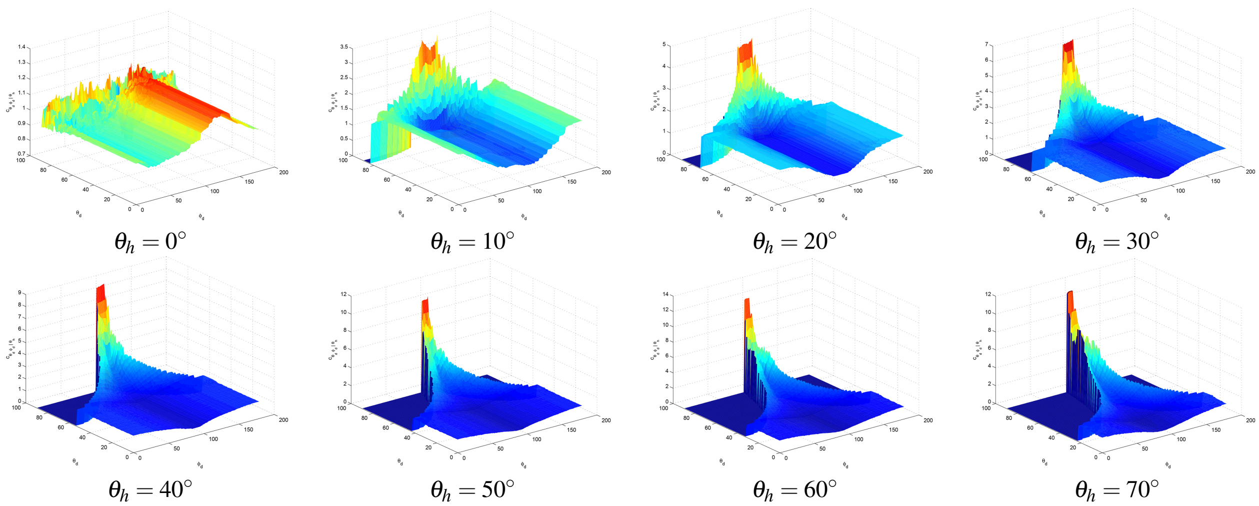

Figure 2: 2D $c_{\theta_d\phi_d|\theta_h}$ distributions of measured dark-red-paint material for various θ_h angles (red channel).

Here $f(x_1|x_2,x_3)$ can be written as:

$$f(x_1|x_2,x_3) = c_{12|3}\{F(x_1|x_3),F(x_2|x_3)\}f(x_1|x_3), \tag{12}$$

or

$$f(x_1|x_2,x_3) = c_{13|2}\{F(x_1|x_2),F(x_3|x_2)\}f(x_1|x_2). \tag{13}$$

Generalization of the conditional pdf and conditional distribution functions using copula distribution can be made using the following relationships, respectively,

$$f(x|\mathbf{v}) = c_{xv_j|\mathbf{v}_{-j}}\{F(x|\mathbf{v}_{-j}),F(v_j|\mathbf{v}_{-j})\}f(x|\mathbf{v}_{-j}), \tag{14}$$

and

$$F(x|\mathbf{v}) = \frac{\partial C_{xv_j|\mathbf{v}_{-j}}\{F(x|\mathbf{v}_{-j}),F(v_j|\mathbf{v}_{-j})\}}{\partial F(v_j|\mathbf{v}_{-j})}, \tag{15}$$

where $\mathbf{v}$ is a n-dimensional vector of random variables $\mathbf{X} = (X_1,X_2,...,X_n)$, v_j is one arbitrarily chosen component of $\mathbf{v}$, $\mathbf{v}_{-j}$ denotes the $\mathbf{v}$ vector excluding v_j component and the form $F(x|\mathbf{v})$ are the marginal conditional distributions.

An advantage of expressing distributions in terms of pair-copulae is that some of the pairs can be ignored to simplify the underlying representation. For example, if a 3D pdf f with random variables X_1,X_2 and X_3 is given, and X_1,X_3 are independent given that X_2, then $c_{13|2}\{F(x_1|x_2),F(x_3|x_2)\} = 1$. Thus, the joint pdf can be expressed as:

$$f(x_1,x_2,x_3) = c_{12}\{F_1(x_1),F_2(x_2)\}c_{23}\{F_2(x_2),F_3(x_3)\}\prod_{i=1}^{3} f_i(x_i). \tag{16}$$

4 BRDF Representation Using Pair-Copula Constructions

In this work isotropic measured BRDF data of Matusik et al. [2003] is modeled using pair-copulae and wavelet decompositions. The measured data is parameterized using the Rusinkiewicz [1998] coordinate system. The Rusinkiewicz parameterization depends on θ_h,ϕ_h,θ_d and ϕ_d. It is well-known that isotropic BRDF values are independent of ϕ_h. Therefore the measured BRDF data of Matusik et al. [2003] is represented as a function of three variables, namely θ_h,θ_d and ϕ_d.

The measured BRDF data is sampled at $90,90,180$ resolutions for θ_h,θ_d and ϕ_d, respectively giving total of $90\times 90\times 180 = 1.458.000$ samples per color channel (Red-Green-Blue). Each bin is obtained at a dense grid with every δ_{θ_h}, δ_{θ_d} and δ_{ϕ_d} degrees of spacing in the intervals $0° \le \theta_h < 90°$, $0° \le \theta_d < 90°$ and $0° \le \phi_d < 180°$, respectively. Since we assume that the BRDF $\rho(\omega_i,\omega_o)$ can be viewed as a multivariate pdf, then we can treat the measured BRDF values as the sampled densities after a simple transformation on the measured BRDFs such that the volume of the empirical density is equal to 1. The scaled BRDF b_{ijk} is evaluated with the following expression:

$$b_{ijk} = \frac{b^*_{ijk}}{K}, \tag{17}$$

where b^*_{ijk} is the measured BRDF with coordinates (i,j,k), $i = 1,2,...,n$, $j = 1,2,...,m$ and $k = 1,2,...,r$, and $K = \delta_{\theta_h}\delta_{\theta_d}\delta_{\phi_d}\sum_{i=1}^{n}\sum_{j=1}^{m}\sum_{k=1}^{r} b^*_{ijk}$ is the scaling factor. The data matrix for the normalized BRDFs is organized as follows

$$\mathbf{B} = \{b_{ijk},\theta_h^{(i)},\theta_d^{(j)},\phi_d^{(k)}\}, \tag{18}$$

where the superscripts in the brackets stand for the bin number of the corresponding angle.

After the scaling transformation, the normalized BRDF, b_{ijk} can be modeled in terms of pair-copulae as:

$$\begin{aligned} b_{ijk} &= f_{\theta_h}(\theta_h^i)f_{\theta_d}(\theta_d^j)f_{\phi_d}(\phi_d^k)c_{\theta_h\theta_d}\{F_{\theta_h}(\theta_h^i),F_{\theta_d}(\theta_d^j)\} \\ &\quad c_{\theta_h\phi_d}\{F_{\theta_h}(\theta_h^i),F_{\phi_d}(\phi_d^k)\} \\ &\quad c_{\theta_d\phi_d|\theta_h}\{F(\theta_d^j|\theta_h^i),F(\phi_d^k|\theta_h^i)\}, \end{aligned} \tag{19}$$

or

$$\begin{aligned} b_{ijk} &= f_{\theta_h}(\theta_h^i)f_{\theta_d}(\theta_d^j)f_{\phi_d}(\phi_d^k)c_{\theta_d\phi_d}\{F_{\theta_d}(\theta_d^j),F_{\phi_d}(\phi_d^k)\} \\ &\quad c_{\theta_h\theta_d}\{F_{\theta_h}(\theta_h^i),F_{\theta_d}(\theta_d^j)\} \\ &\quad c_{\phi_d\theta_h|\theta_d}\{F(\phi_d^k|\theta_d^j),F(\theta_h^i|\theta_d^j)\}, \end{aligned} \tag{20}$$

or

$$\begin{aligned} b_{ijk} \quad = \quad & f_{\theta_h}(\theta_h^i) f_{\theta_d}(\theta_d^j) f_{\phi_d}(\phi_d^k) c_{\theta_h\phi_d}\{F_{\theta_h}(\theta_h^i), F_{\phi_d}(\phi_d^k)\} \\ & c_{\theta_d\phi_d}\{F_{\theta_d}(\theta_d^j), F_{\phi_d}(\phi_d^k)\} \\ & c_{\theta_h\theta_d|\phi_d}\{F(\theta_d^j|\phi_d^k), F(\theta_d^j|\phi_d^k)\}. \qquad (21) \end{aligned}$$

In Equation 19, the conditional copula distribution $c_{\theta_d\phi_d|\theta_h}$ is a 2D distribution but it should be stored for each θ_h. Therefore storing these distributions for BRDF representation will be inefficient. The same data storage problem is valid for $c_{\phi_d\theta_h|\theta_d}$ in Equation 20 and $c_{\theta_h\theta_d|\phi_d}$ in Equation 21. Since we would like to generalize the notation, we symbolize $c_{\theta_d\phi_d|\theta_h}$, $c_{\phi_d\theta_h|\theta_d}$, and $c_{\theta_h\theta_d|\phi_d}$ as $c_{xy|z}$. Accordingly, using uniformly distributed data corresponding to $c_{xy|z}$ will improve compression ratios of the 3D data. The function values of $c_{xy|z}$ are equal to 1 when x and y are independent [Aas et al. 2009].

For choosing the most appropriate expression out of three equations in Equation 19, Equation 20 and Equation 21, first we represented BRDF assuming that $c_{xy|z} = 1$. Each measured BRDF data is then approximated using all possible pair-copula decompositions and the corresponding absolute error is evaluated. Our empirical results showed that among the others $c_{\theta_d\phi_d|\theta_h}$ is approximately uniformly distributed for almost all materials. These results indicate that θ_d and ϕ_d are nearly independent for a given θ_h.

After choosing the most appropriate distribution, the contribution of θ_h to the goodness-of-fit of the model is investigated. It is seen from Figure 1 that sum of absolute errors between the estimated BRDFs and measured BRDFs are greater in the $(0, \pi/4)$ region than that of the region $(\pi/4, \pi/2)$.

In Figure 1, the 2D distributions $c_{\theta_d\phi_d|\theta_h}$ have the largest error values between the first 45 degrees of θ_h. Highest fitting errors were observed for $\theta_h < 45^\circ$ for most of the materials. After the 45 degrees the distribution are nearly similar. This situation can be seen on Figure 2.

5 Estimation

Empirical marginal distributions are obtained from the normalized data as follows:

$$\hat{f}_{\theta_h}^i = b_{i..} = \sum_{j=0}^{89} \sum_{k=0}^{179} b_{ijk}, \qquad (22)$$

$$\hat{f}_{\theta_d}^j = b_{.j.} = \sum_{i=0}^{89} \sum_{k=0}^{179} b_{ijk}, \qquad (23)$$

$$\hat{f}_{\phi_d}^k = b_{..k} = \sum_{i=0}^{89} \sum_{j=0}^{89} b_{ijk}. \qquad (24)$$

Using the univariate marginal probability densities $\hat{f}_{\theta_h}$, $\hat{f}_{\theta_d}$ and $\hat{f}_{\phi_d}$, the copula densities $c_{\theta_h\theta_d}\{F_{\theta_h}(\theta_h^i), F_{\theta_d}(\theta_d^j)\}$ and $c_{\theta_h\phi_d}\{F_{\theta_h}(\theta_h^i), F_{\phi_d}(\phi_d^k)\}$ can be constructed using the following relationships:

$$\hat{c}_{\theta_h\theta_d} = \frac{\hat{f}_{\theta_h\theta_d}}{\hat{f}_{\theta_h}\hat{f}_{\theta_d}}, \qquad (25)$$

where $\hat{f}_{\theta_h\theta_d}$ is the marginal density evaluated as

$$\hat{f}_{\theta_h^i\theta_d^j} = \sum_{k=0}^{179} b_{ijk}, \qquad (26)$$

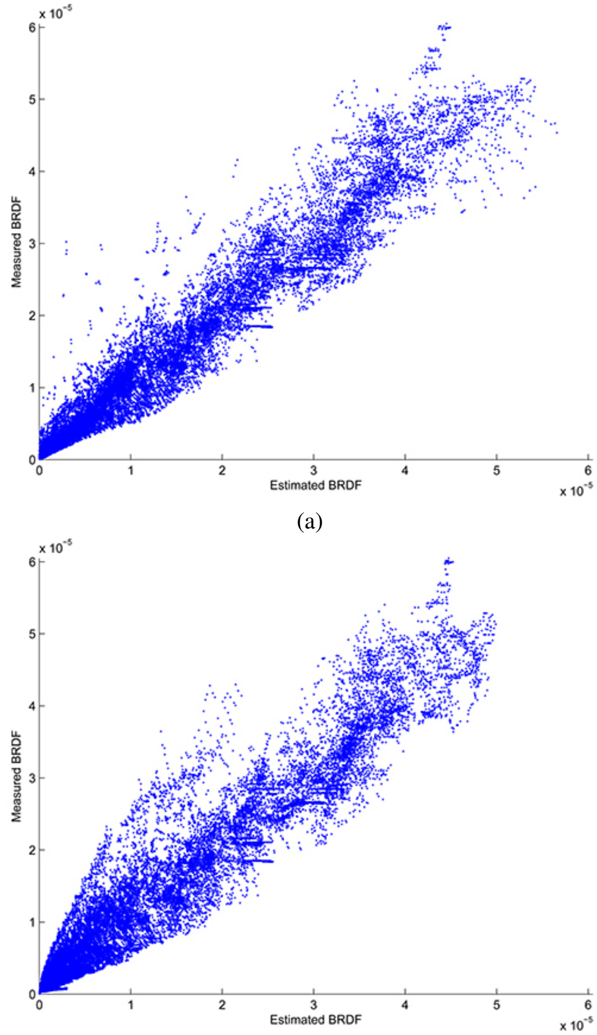

(a)

(b)

Figure 3: Plots of red channel of measured BRDFs of dark-red-paint against the estimated values based on pair-copula and wavelet decomposition. (a) Fitted terms are evaluated using $c_{\theta_d\phi_d|\theta_h}$ as it is, (b) Fitted terms are evaluated using $c_{\theta_d\phi_d|\theta_h} = 1$.

and

$$\hat{c}_{\theta_h\phi_d} = \frac{\hat{f}_{\theta_h\phi_d}}{\hat{f}_{\theta_h}\hat{f}_{\phi_d}}, \qquad (27)$$

where $\hat{f}_{\theta_h\phi_d}$ is the marginal density evaluated as

$$\hat{f}_{\theta_h^i\phi_d^k} = \sum_{j=0}^{89} b_{ijk}. \qquad (28)$$

The 2D $\hat{c}_{\theta_h\theta_d}$ and $\hat{c}_{\theta_h\phi_d}$ copula densities are estimated by employing the wavelet decomposition technique described in Genest et al. [2009]. The Haar wavelets [Graps 1995] are used for decomposition and only the low frequency details (approximation) are stored in the second level with a compression ratio of 1/16.

The final step consists of decomposing the $c_{\theta_d\phi_d|\theta_h}$ copula density given in Equation 19. The results of fitting with and without $c_{\theta_d\phi_d|\theta_h}$ term are shown in Figure 3. In this figure, the fitted BRDFs are

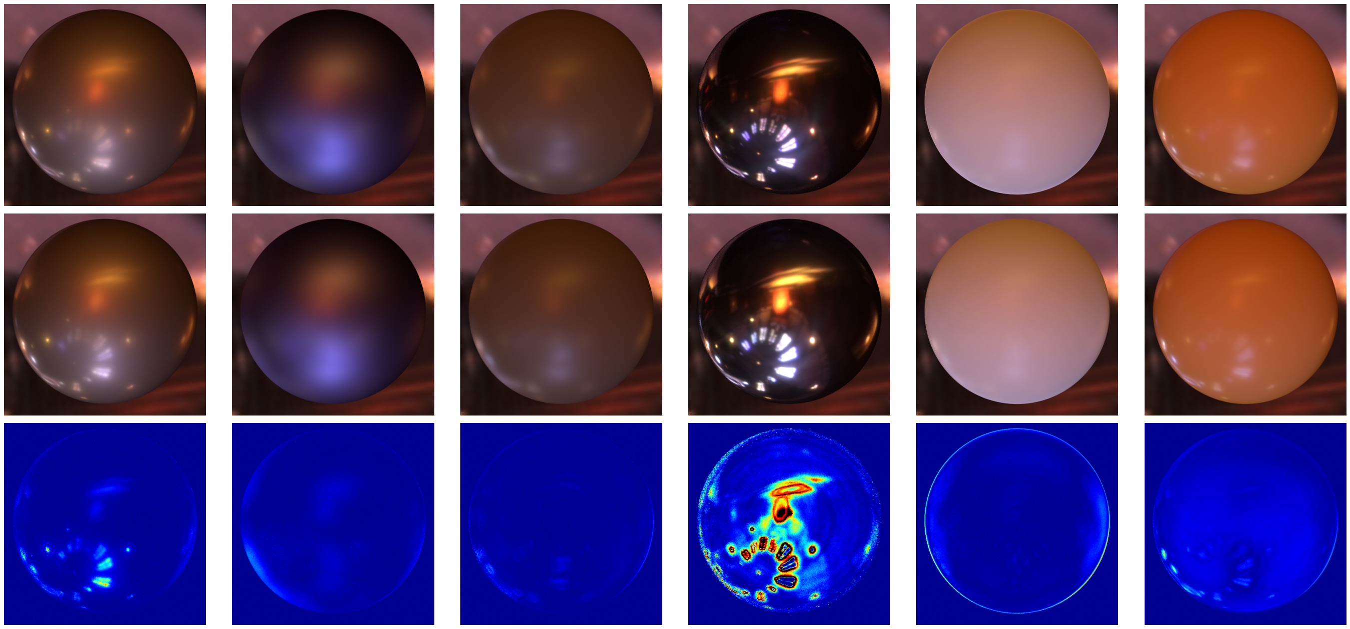

(a) (b) (c) (d) (e) (f)

Figure 4: Various spheres rendered with pair-copula and wavelet decomposition using different materials. Columns left to right: alum-bronze (PSNR=39.63), blue-metallic-paint (PSNR=43.16), fruitwood-241 (PSNR=45.74), chrome-steel (PSNR=26.77), delrin (PSNR=39.38) and yellow-matte-plastic (PSNR=37.66). Rows top to bottom: Reference images rendered using measured data; images rendered using pair-copula and wavelet decomposition and difference false color images scaled by a factor of 1.5.

plotted against the measured BRDF values. As it is seen from Figure 3 that the fitting quality improved considerably when $c_{\theta_d\phi_d|\theta_h}$ term is included. Apparently inclusion of this term in the model has a significant effect on the accuracy of the model. However a compression with a high ratio can be achieved using low frequency terms and higher levels of wavelet decomposition.

For each given θ_h^i, the corresponding copula densities can be estimated as:

$$\hat{c}_{\theta_d^j\phi_d^k|\theta_h^i} = \frac{\hat{c}_{\theta_d^j\phi_d^k|\theta_h^i}}{\hat{f}_{\theta_d^j|\theta_h^i}\hat{f}_{\phi_d^k|\theta_h^i}}. \tag{29}$$

In this work, these 2D densities are decomposed using the well-known Daubechies wavelets [Graps 1995]. We used Daubechies-4-tap wavelets to decompose the 2D densities. For each given θ_h^i, these 2D densities are decomposed into three levels and only the approximation coefficients are stored with a compression ratio of 1/64.

For further compression, we looked at the errors for each given θ_h^i. As shown in Figure 1, the errors in the first half are greater than the second half of entire region. It is seen from the Figure 2 that bivariate distributions become very similar to each other, when θ_h is greater than 40 degrees. We used this redundancy to improve the compression ratio of BRDF data.

To render a color image at a given outgoing direction, we applied the wavelet decomposition of the copula density to the normalized mean values of measured BRDFs of the three color channels. Following a similar approach that was used by Ngan et al. [2005], we estimated the diffuse and specular parameters for each pair of measured BRDF of each color channel and the approximated BRDF values using a robust linear regression procedure [DuMouchel and O'Brien 1989].

6 Importance Sampling

Importance sampling is a variance reduction technique in Monte Carlo rendering. If the samples are chosen from the right BRDF distribution, the variance decreases significantly. Therefore sampling of the BRDF distribution is an important issue in rendering [Jensen et al. 2003].

In Monte Carlo rendering algorithms, outgoing radiance $L_o(\theta_o,\phi_o)$ is estimated using the following formula:

$$L_o(\theta_o,\phi_o) = \frac{1}{N}\sum_{s=1}^{N} L_i(\theta_s,\phi_s)\frac{\rho(\theta_s,\phi_s,\theta_o,\phi_o)\cos\theta_s\sin\theta_s}{p_i(\theta_s,\phi_s \mid \theta_o,\phi_o)}, \tag{30}$$

where N is the number of samples, L_i is the incoming radiance, ρ is the BRDF described in Equation 1, $\vec{\omega}_s = \{(\theta_s,\phi_s)\}$ is the sampling direction vector, and p_i is the conditional distribution of θ_s and ϕ_s given that θ_o and ϕ_o.

For our representation, deriving an efficient importance sampling procedure is not trivial. Because our BRDF representation is based on Rusinkiewicz [1998] coordinate system, and importance sampling should be made in standard coordinate system. We could generate samples in Rusinkiewicz [1998] coordinate system, and transform them into standard coordinate system

$$p_i(\theta_i,\phi_i \mid \theta_o,\phi_o) = \frac{p_h(\theta_h,\phi_h,\theta_d,\phi_d)|J|}{p_o(\theta_o,\phi_o)}, \tag{31}$$

using the Jacobian (J) of the underlying change of variables if we knew its proper value. However, calculation of the Jacobian is not trivial. In Equation 31, p_h is the 4D pdf described in Rusinkiewicz [1998] coordinate system, p_i is the 2D conditional

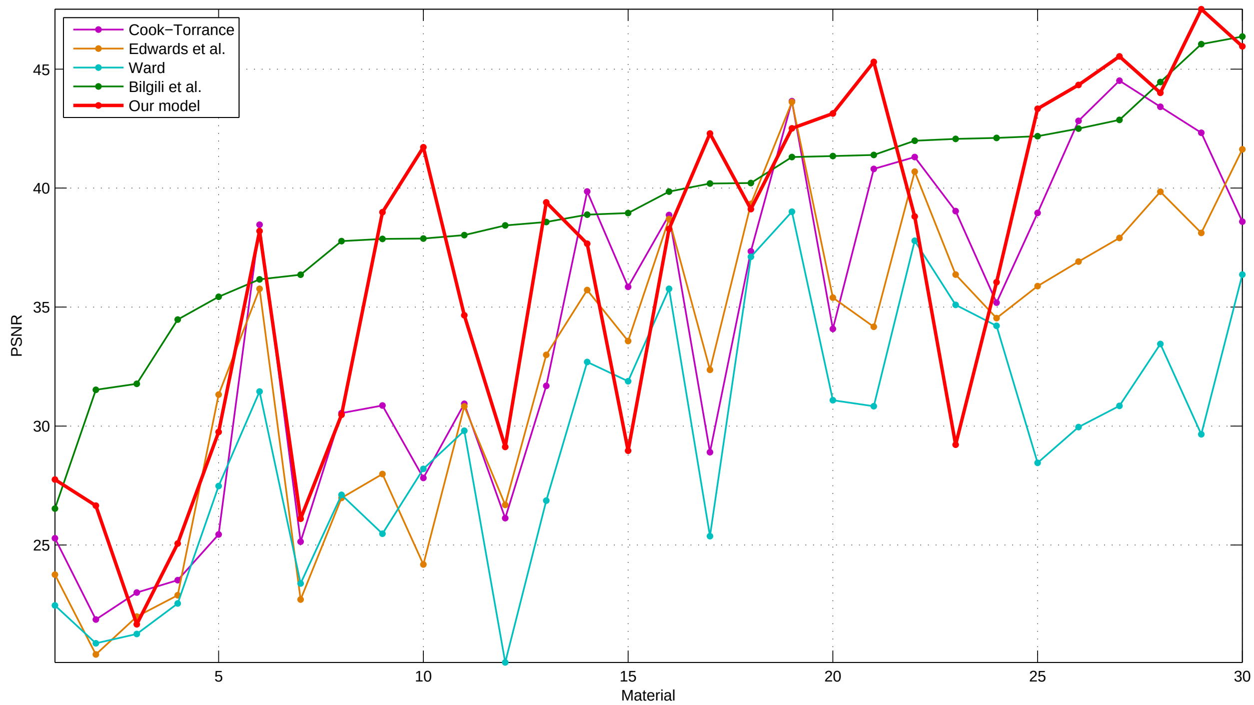

Figure 5: The PSNR values of five BRDF representations for randomly selected 30 isotropic materials from MERL MIT database. The PSNR values are sorted in the PSNRs of the Bilgili et al. model (Green) for better visualization. Our model gives the highest PSNR values in 11 out of 30 randomly selected materials.

pdf, and p_o is the 2D pdf. Both p_i and p_o are described in the standard coordinate system.

In order to develop a sampling procedure, we can use the standard coordinate system instead of Rusinkiewicz [1998] coordinate system in the sampling function of our BRDF representation. According to that, we represent $p_i(\theta_i, \phi_i \mid \theta_o, \phi_o)$ as:

$$p_i(\theta_i, \phi_i \mid \theta_o, \phi_o) = \frac{\rho(\theta_i, \phi_i, \theta_o, \phi_o)}{p_o(\theta_o, \phi_o)}, \quad (32)$$

where ρ is the BRDF described in Equation 1, p_o is 2D pdf. Then, we model ρ and p_o using pair-copula constructions and wavelet transforms. The computational cost of this sampling procedure is very expensive since generating incoming vectors from this 2D conditional pdf is not efficient. On the other hand, for reducing time required for Monte Carlo integration, some optimizations and approximations can be made to this sampling procedure and this sampling function, respectively.

7 Results

We have tested our model on 30 randomly chosen measured isotropic BRDF data from MERL MIT database [Matusik et al. 2003]. The results of the 6 materials are presented in Figure 4. The renderings of spheres shown in Figure 4 are acquired using the Physically Based Rendering Toolkit (PBRT) [Pharr and Humphreys 2004] using the direct illumination option.

It is seen from Figure 4 that pair-copula constructions [Aas et al. 2009] and wavelet transforms have provided images with a satisfactory visual quality. We used Peak Signal to Noise Ratio (PSNR) [Richardson 2002] for quantitative comparisons of rendered spheres with the original rendered spheres. Higher PSNR values indicate better approximations. As seen from Figure 4 that, specular materials have lower PSNR values than those of diffuse and glossy materials. This is possibly caused by the measurement errors in these materials in the specular areas ($\theta_i > 80°$ or $\theta_o > 80°$). This situation has also been reported by Ngan et al. [2005].

We have compared our model with various BRDF models, namely Cook-Torrance BRDF model [Cook and Torrance 1981], Edwards et al. BRDF model [Edwards et al. 2006], Ward BRDF model [Ward 1992], and Bilgili et al. BRDF model [Bilgili et al. 2011]. The PSNR values of these BRDF models based on fittings of 30 randomly selected measured BRDF data from MERL MIT database [Matusik et al. 2003] are shown in Figure 5. It is seen from Figure 5 that our model gives the highest PSNR values in 11 materials and it can be seen as a good alternative to represent isotropic materials accurately.

Based on the data set [Matusik et al. 2003] we used, we need to store 60.4 KB data for each material, which requires 33 MB storage space. According to that, our compression technique compressed the data up to about $1/600$ of its original size. The results have shown that, it is possible to model any multivariate distribution using the interactions between each pair of random variables. The proposed technique also lends itself to identify the variables which can be considered as approximately independent.

8 Conclusions and Future Work

In this paper, we introduced a compact technique to represent BRDF data using pair-copula constructions and wavelet transforms. Our technique also can be generalized for compression of data from any multivariate distribution. To illustrate the quality of resulting approximations, we have rendered spheres for various isotropic materials, and compared the proposed BRDF representation with a number of well-known BRDF models. It is empirically shown that the proposed technique has provided satisfactory results.

A major drawback of this approach is that the computational cost of wavelet transforms depends on the level of decomposition. Although high level compressions are satisfactory for most practical applications, high quality renderings can be achieved only with low compression ratios.

As a future work, it can be shown that this compression technique can be generalized to higher dimensional problems such as Bidirectional Subsurface Scattering Reflection Distribution Functions (BSSRDFs). We also would like to represent 4D measured anisotropic BRDF data with our representation.

Acknowledgements

We would like to thank the anonymous reviewers for their thoughtful comments and Wojciech Matusik et al. [2003] for using their measured BRDF data (from the MERL MIT database).

References

AAS, K., CZADO, C., FRIGESSI, A., AND BAKKEN, H. 2009. Pair-copula constructions of multiple dependence. *Insurance: Mathematics and Economics 44*, 2, 182 – 198.

AKENINE-MÖLLER, T., HAINES, E., AND HOFFMAN, N. 2008. *Real-Time Rendering 3rd Edition*. A. K. Peters, Ltd., Natick, MA, USA.

ASHIKHMIN, M., AND SHIRLEY, P. 2000. An anisotropic Phong BRDF model. *Journal of Graphics Tools 5*, 2, 25–32.

BILGILI, A., ÖZTÜRK, A., AND KURT, M. 2011. A general brdf representation based on tensor decomposition. *Computer Graphics Forum 30*, 8 (December), 2427–2439.

BLINN, J. F. 1977. Models of light reflection for computer synthesized pictures. *SIGGRAPH Computer Graphics 11*, 2, 192–198. (Proceedings of SIGGRAPH 77).

COOK, R. L., AND TORRANCE, K. E. 1981. A reflectance model for computer graphics. *SIGGRAPH Computer Graphics 15*, 3, 307–316. (Proceedings of SIGGRAPH 81).

DUMOUCHEL, W. H., AND O'BRIEN, F. L. 1989. Integrating a robust option into a multiple regression computing environment. In *Computing Science and Statistics: Proceedings of the 21st Symposium on the Interface*, American Statistical Association, Alexandria, VA, K. Berk and L. Malone, Eds., 297–301.

DÜR, A. 2006. An improved normalization for the ward reflectance model. *Journal of Graphics Tools 11*, 1, 51–59.

EDWARDS, D., BOULOS, S., JOHNSON, J., SHIRLEY, P., ASHIKHMIN, M., STARK, M., AND WYMAN, C. 2006. The halfway vector disk for brdf modeling. *ACM Trans. Gr. 25*, 1 (Jan.), 1–18.

GEISLER-MORODER, D., AND DÜR, A. 2010. A new ward brdf model with bounded albedo. *Computer Graphics Forum 29*, 4 (June), 1391–1398. (Proceedings of Eurographics Symposium on Rendering 2010).

GENEST, C., MASIELLO, E., AND TRIBOULEY, K. 2009. Estimating copula densities through wavelets. *Insurance: Mathematics and Economics 44*, 2 (April), 170–181.

GRAPS, A. 1995. An introduction to wavelets. *Computing in Science and Engineering 2*, 50–61.

HE, X. D., TORRANCE, K. E., SILLION, F. X., AND GREENBERG, D. P. 1991. A comprehensive physical model for light reflection. *SIGGRAPH Computer Graphics 25*, 4, 175–186. (Proceedings of SIGGRAPH 91).

JENSEN, H. W., ARVO, J., DUTRE, P., KELLER, A., OWEN, A., PHARR, M., AND SHIRLEY, P. 2003. Course 44: Monte carlo ray tracing. In *ACM SIGGRAPH 2003 Full Conference DVD-ROM*, H. W. Jensen, Ed.

LAFORTUNE, E. P., FOO, S.-C., TORRANCE, K. E., AND GREENBERG, D. P. 1997. Non-linear approximation of reflectance functions. In *Proceedings of SIGGRAPH 97*, ACM Press/Addison-Wesley Publishing Co., New York, NY, USA, 117–126.

LAWRENCE, J., RUSINKIEWICZ, S., AND RAMAMOORTHI, R. 2004. Efficient BRDF importance sampling using a factored representation. *ACM Trans. Gr. 23*, 3, 496–505. (Proceedings of SIGGRAPH 2004).

MATUSIK, W., PFISTER, H., BRAND, M., AND MCMILLAN, L. 2003. A data-driven reflectance model. *ACM Trans. Gr. 22*, 3 (July), 759–769. (Proceedings of SIGGRAPH 2003).

NELSEN, R. B. 2006. *An Introduction to Copulas (Springer Series in Statistics)*. Springer-Verlag New York, Inc., Secaucus, NJ, USA.

NGAN, A., DURAND, F., AND MATUSIK, W. 2005. Experimental analysis of brdf models. In *Proceedings of Eurographics Symposium on Rendering*, Eurographics Association, Konstanz, Germany, K. Bala and P. Dutré, Eds., 117–126.

NICODEMUS, F. E., RICHMOND, J. C., HSIA, J. J., GINSBERG, I. W., AND LIMPERIS, T. 1977. Geometrical considerations and nomenclature for reflectance. Monograph, National Bureau of Standards (US), Oct.

OREN, M., AND NAYAR, S. K. 1994. Generalization of lambert's reflectance model. In *Proceedings of SIGGRAPH 94*, ACM, New York, NY, USA, 239–246.

ÖZTÜRK, A., KURT, M., AND BILGILI, A. 2010. A copula-based brdf model. *Computer Graphics Forum 29*, 6 (September), 1795–1806.

PHARR, M., AND HUMPHREYS, G. 2004. *Physically Based Rendering: From Theory to Implementation*. Morgan Kaufmann Publishers Inc., San Francisco, CA, USA.

PHONG, B. T. 1975. Illumination for computer generated pictures. *Commun. ACM 18*, 6 (June), 311–317.

RICHARDSON, I. E. 2002. *Video Codec Design: Developing Image and Video Compression Systems*. John Wiley & Sons, Inc., New York, NY, USA.

RUSINKIEWICZ, S. M. 1998. A new change of variables for efficient brdf representation. In *Proceedings of Eurographics Workshop on Rendering*, Springer, Vienna, Austria, G. Drettakis and N. L. Max, Eds., 11–22.

WARD, G. J. 1992. Measuring and modeling anisotropic reflection. *SIGGRAPH Computer Graphics 26*, 2, 265–272. (Proceedings of SIGGRAPH 92).